Università degli Studi di Napoli "Federico II"

SCUOLA POLITECNICA E DELLE SCIENZE DI BASE

DIPARTIMENTO DI INGEGNERIA INDUSTRIALE

CORSO DI LAUREA IN INGEGNERIA AEROSPAZIALE

CLASSE DELLE LAUREE IN INGEGNERIA INDUSTRIALE (L-9)

Elaborato di laurea in Meccanica del Volo

Geometric modelling and analysis of performance, stability, and control of the Boeing 737 NG aircraft family

Relatore:
Prof. Danilo Ciliberti

Candidato:
Edoardo Vincenti
Matr. N35003471

ANNO ACCADEMICO 2022 – 2023

Abstract

The purpose of this work is to model the Boeing 737 NG aircraft family using JPAD software, followed by performance analysis using MATLAB code, and stability and control analysis using the OpenVSP suite. JPAD (Java toolchain of Programs for Aircraft Design) is an integrated and comprehensive software that supports aircraft design, providing a user-experience designed to assist the designer throughout the entire process, from aircraft specifications to multidisciplinary analysis and optimization. OpenVSP is an open-source parametric tool for aircraft geometry originally developed by NASA. OpenVSP allows the creation of 3D aircraft models and provides support for engineering analysis of these models.

Another crucial tool used in this study is VSPAERO, a fast, linear, and grid-based vortex solver. VSPAERO is employed for aircraft stability analysis. This solver applies discrete vortices to each panel generated in the aircraft geometry file created with OpenVSP. Subsequently, it evaluates the vortices over the entire aircraft surface to obtain a pressure distribution and, consequently, aerodynamic forces.

Sommario

Il presente lavoro ha come obiettivo la modellazione della famiglia di velivoli Boeing 737 NG, utilizzando il software JPAD, a cui segue l’analisi delle prestazioni con l’utilizzo di un codice MATLAB e della stabilità e del controllo con la suite OpenVSP. JPAD (Java toolchain of Programs for Aircraft Design) è un software integrato e completo che supporta la progettazione di aeromobili, offrendo una user-experience pensata per accompagnare il progettista lungo l'intero processo, dalle specifiche dell'aeromobile all'analisi e all'ottimizzazione multidisciplinare. OpenVSP è uno strumento parametrico open source per la geometria dei velivoli originariamente sviluppato dalla NASA. OpenVSP consente la creazione di modelli 3D di aeromobili e fornisce supporto per l'analisi ingegneristica di tali modelli. Un altro strumento cruciale utilizzato in questo lavoro è VSPAERO, un solutore veloce, lineare e a reticolo di vortici. VSPAERO viene impiegato per l'analisi di stabilità del velivolo. Questo solutore applica vortici discreti a ciascun pannello generato nel file di geometria del velivolo creato con OpenVSP. Successivamente, valuta i vortici sull'intera superficie del velivolo per ottenere una distribuzione della pressione e, di conseguenza, delle forze aerodinamiche.

Summary

List of figures

List of tables

1 Introduction

1.1 Objectives

The objective of this thesis work is the geometric modeling and analysis of the performance, stability, and control of the Boeing 737 NG aircraft family.

1.2 Boeing 737 NG aircraft family

The 737 is a short to medium-range aircraft that embodies the Boeing philosophy: providing airlines with added value through reliable, straightforward, cost-effective, and maintainable products.

The 737 Next Generation is manufactured in four distinct variants: the 737-600, 737-700, 737-800, and 737-900, with seating capacities ranging from 132 to 215.

Figure 1.1 - Example of Boeing 737-800

These models, compared to their predecessors, feature a new wing that enhances efficiency and allows for the installation of larger fuel tanks, resulting in increased flight range.

These aircraft employ a modification procedure known as "fuselage stretching". It is a complex process that involves lengthening the fuselage of an existing aircraft to increase passenger or cargo capacity. This modification is carried out to improve the performance and efficiency of the aircraft. The process includes design and analysis, fuselage cutting, insertion of an additional section called a "plug", structural reinforcement, system integration, testing, and certification. Fuselage stretching provides a cost-effective alternative to purchasing new aircraft and has allowed manufacturers to enhance the capabilities and efficiency of their aircraft.

The range is approximately 6000 km, which represents a 38% increase compared to the previous versions.

The advanced aerodynamic profile of the wing enables the aircraft to maintain a cruise speed of 0.785 Mach, compared to the 0.745 Mach of the previous 737 models. The maximum allowable speed is 0.82 Mach.

The engines of the 737 NG are the CFM56-7, manufactured by CFMI. The acoustic emissions are below "Stage 3" limits. These engines are known for their low fuel consumption and reduced maintenance costs.

The maximum cruise altitude for the 737 NG is 12500 meters (41000 ft).

1.3 Software

This work is based, first and foremost, on the use of JPAD, a software developed by SmartUp Engineering s.r.l., which allows for the creation of a highly realistic 3d model by inputting data of the aircraft's main components. Additionally, this software enables the export of the created model in various formats, particularly OPENVSP, used for stability analyses with the OPENVSP-VSPAERO software, an open-source software developed by NASA.

For performance studies, MATLAB code is utilized, utilizing specific functions included in the 'Aerospace Toolbox' add-on.

2 JPAD Modeller

The first step to initiate the modelling process consists of searching for the geometric data of the main aircraft components to be inserted into the JPAD software. Some data, such as area, aspect ratio, and length of the main parts of the aircraft, have been obtained from reliable sources, while all other geometric data have been extracted from the views of the models taken from the Boeing 737 manual, manually measuring the respective element, and maintaining the proportional relationships.

Once all the data has been found, it must be entered into the appropriate section of the software. The interface of the software is divided into two sections. In the left section, there are several subsections where input data for the various considered aircraft components will be placed. In the right part, it is possible to view the generated 3D model of the aircraft from different perspectives (frontal, lateral, top-down).

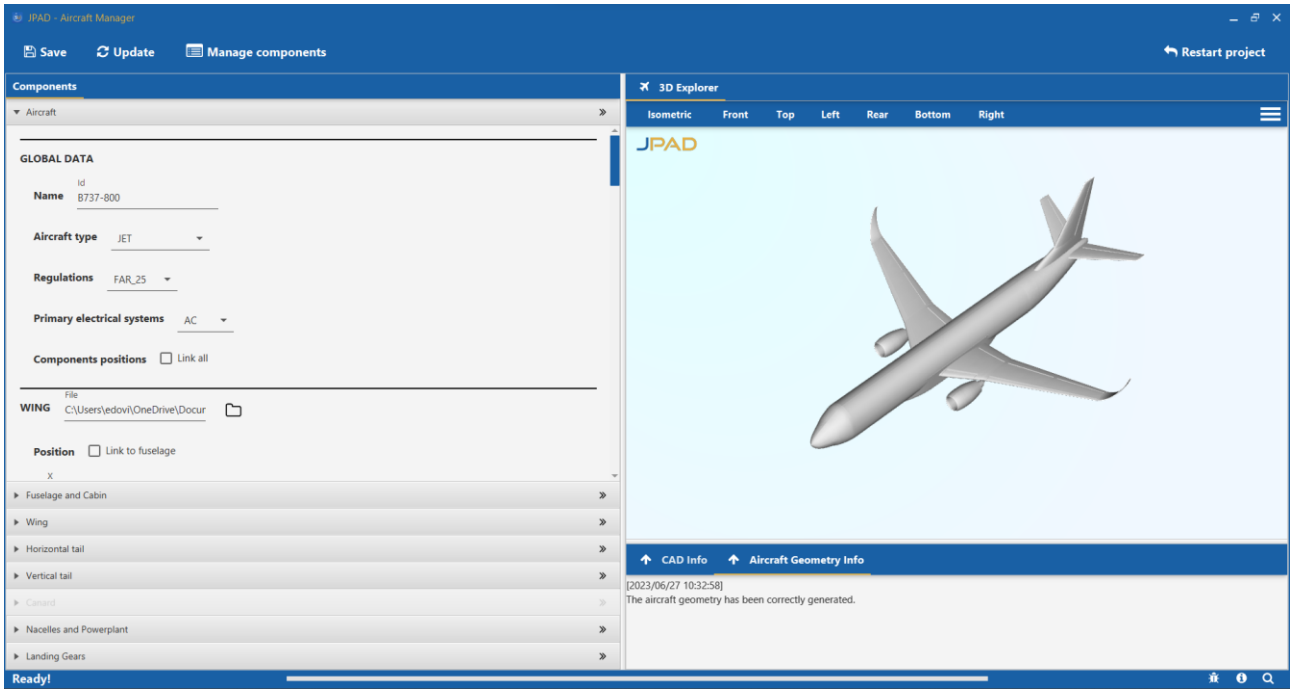

Figure 2.1 - JPAD interface

Regarding the subsections in the left section, they are divided into:

- The “Aircraft” section where the position in the three coordinates (X, Y, Z) of the main aircraft components is determined.
- The “Fuselage and Cabin” section provides access to the set of input parameters defining the external shape of the fuselage and passengers’ accommodation inside the central body of the aircraft. The fuselage is parametrically defined as the union of three separate trunks

(nose, central cylinder, tail), for which differently shaped cross-section can be defined: separate shape coefficients are provided for three main blocks of the fuselage.

- The “Wing” section provides access to the set of input parameters defining the external shape of the wing in terms of a collection of linked panels. In this section, movable surfaces such as flaps, slats, and ailerons can be inserted. In this case, internal flaps with double slotted configuration and external flaps with single slotted configuration are used to improve performance and reduce low-speed noise.
- The "Horizontal Tail" section provides access to a range of input parameters that define the external shape of the horizontal tail. In this section, adjustable components like the elevator can be included.
- The "Vertical Tail" section grants access to a set of input parameters that define the external shape of the vertical tail. In this section, movable surfaces such as the rudder can be incorporated.
- The “Nacelles and Powerplant” section grants users access to a range of input parameters defining the external shape of the nacelle component, as well as the main geometrical engine information and specifications.

On the right side, as input data is entered and the 'Update' button is pressed, the CAD model is updated. Additionally, in this section, it is possible to activate movable surfaces and winglets, generating them in the input parameters area of the 3D model.

Presented below are the collected data for each individual model belonging to the Boeing 737 NG aircraft family. These data are accompanied by the corresponding 3D models generated by the software, showcasing the aircraft from different perspectives.

2.1 Geometric modelling of the Boeing 737-600

The Boeing 737-600 is the smallest aircraft in its family and can accommodate from 108 (two-class configuration) to 123 passengers (single-class configuration).
The primary data of the components of the Boeing 737-600 is compiled in Table 2.1.

Fuselage and Cabine	**Length [m]**	**Length Nose [m]**	**Len. tail [m]**	**Cabin length [m]**	**Equivalent section diameter [m]**			
	29.779	3.99	10.601	15.187	3.76			
Wing	**Area [m^2]**	**Span [m]**	**Aspect ratio**	**Sweep angle [deg]**	**Dihedral angle [deg]**	**C_{root} [m]**	**C_{tip} [m]**	**Movables**
	124.596	34.296	9.441	33 (I panel) 26 (II panel)	6	7.59	1.215	Flaps, Slats and ailerons
Horizontal tail	**Area [m^2]**	**Span [m]**	**Aspect ratio**	**Sweep angle [deg]**	**Dihedral angle [deg]**	**C_{root} [m]**	**C_{tip} [m]**	
	32.306	13.358	5.523	33	10	3.52	1.31	
Vertical tail	**Area [m^2]**	**Span [m]**	**Aspect ratio**	**Sweep angle [deg]**	**Dihedral angle [deg]**	**C_{root} [m]**	**C_{tip} [m]**	
	27.37	7.6	2.11	68(I panel) 37 (II panel)	0	8	1.4	
Nacelles and powerplants	**Engine Type**	**Engine number**	**Max TO weight [kg]**	**Length [m]**	**Nacelle diameter [m]**			
	CFM International CFM56-7	2	65090	4.1	2			

Table 2.1 - Boeing 737-600 data

The final model obtained is as follows:

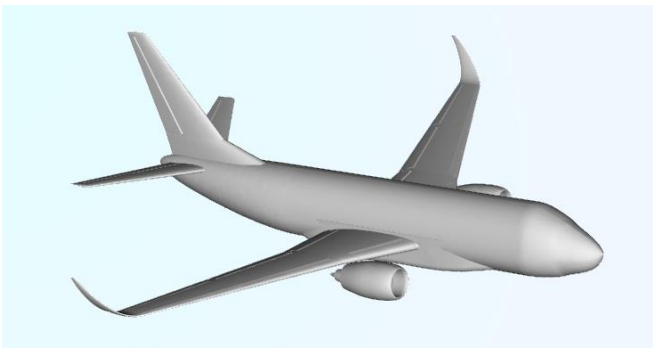

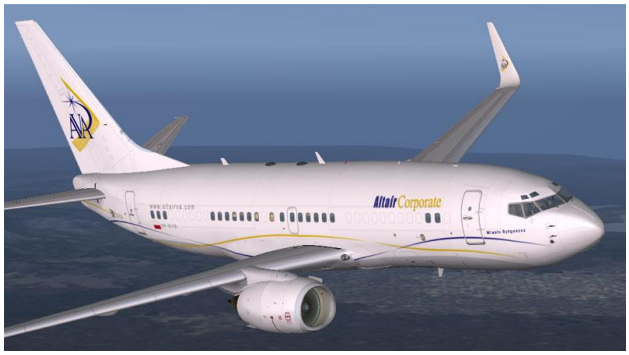

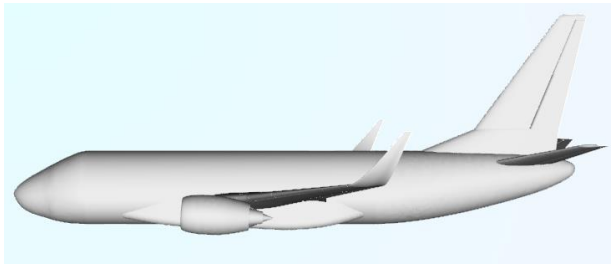

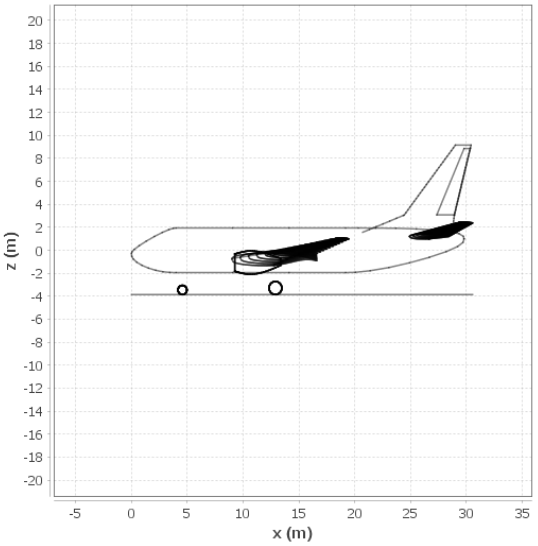

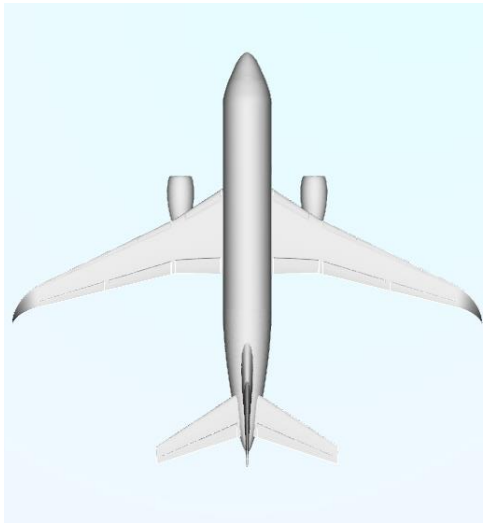

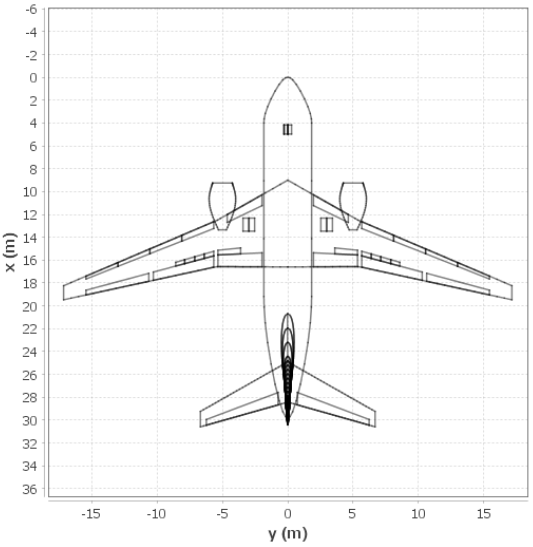

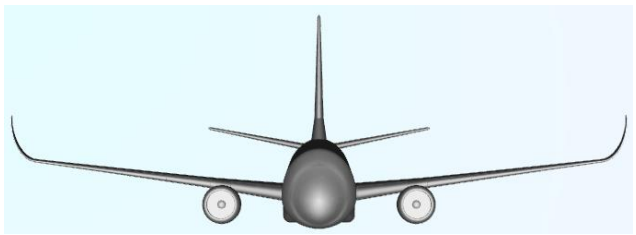

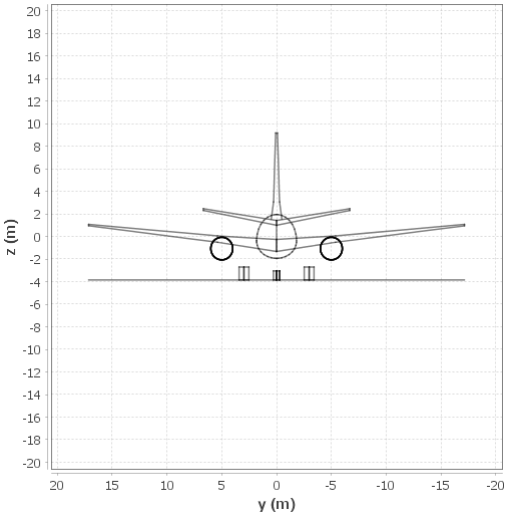

Figure 2.2 - Boeing 737-600 views comparisons

2.2 Geometric modelling of the Boeing 737-700

The Boeing 737-700 is the first to be born in its family and can accommodate from 128 (two-class configuration) to 140 passengers (single-class configuration).

The primary data of the components of the Boeing 737-700 is compiled in Table 2.2.

Fuselage and Cabin	**Length [m]**	**Length Nose [m]**	**Len. tail [m]**	**Cabin length [m]**	**Equivalent section diameter [m]**			
	32.180	3.99	10.601	17.602	3.76			
Wing	**Area [m^2]**	**Span [m]**	**Aspect ratio**	**Sweep angle [deg]**	**Dihedral angle [deg]**	**C_{root} [m]**	**C_{tip} [m]**	**Movables**
	124.596	34.296	9.441	33 (I panel) 26 (II panel)	6	7.59	1.215	Flaps, Slats and aileron
Horizontal tail	**Area [m^2]**	**Span [m]**	**Aspect ratio**	**Sweep angle [deg]**	**Dihedral angle [deg]**	**C_{root} [m]**	**C_{tip} [m]**	
	32.306	13.358	5.523	33	10	3.52	1.31	
Vertical tail	**Area [m^2]**	**Span [m]**	**Aspect ratio**	**Sweep angle [deg]**	**Dihedral angle [deg]**	**C_{root} [m]**	**C_{tip} [m]**	
	27.37	7.6	2.11	68 (I panel) 37 (II panel)	0	8	1.4	
Nacelles and powerplants	**Engine Type**	**Engine number**	**Max TO weight [kg]**	**Length [m]**	**Nacelle diameter [m]**			
	CFM International CFM56-7	2	69400	4.1	2			

Table 2.2 - Boeing 737-700 data

The final model obtained is as follows:

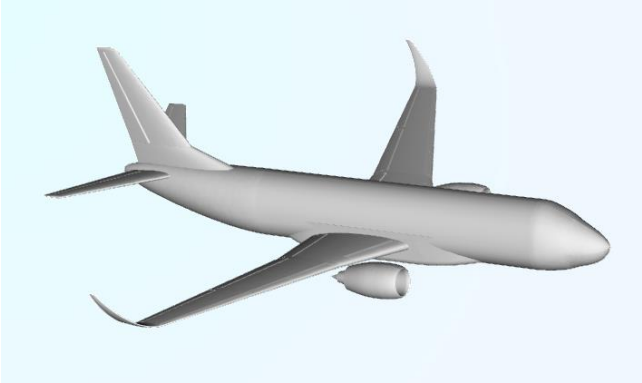

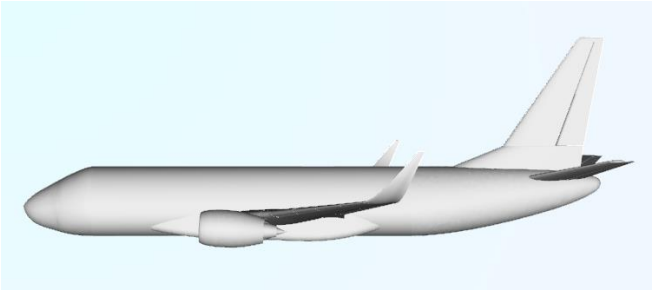

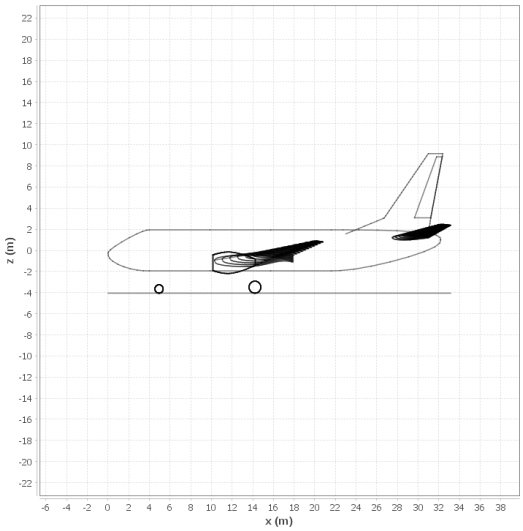

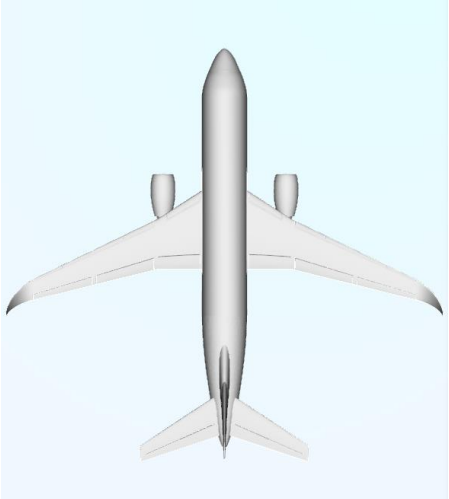

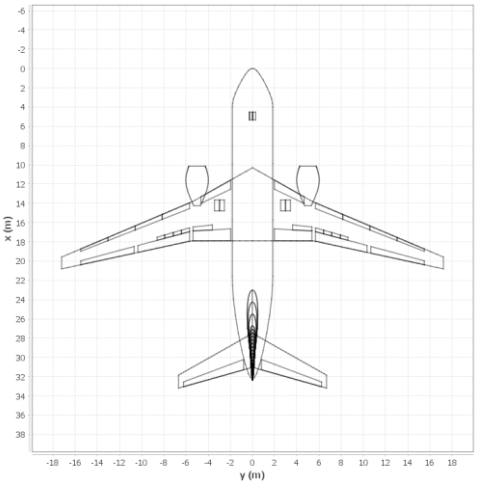

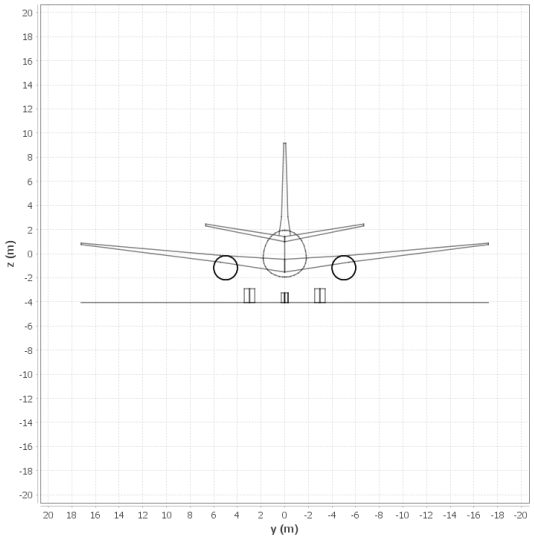

Figure 2.3 - Boeing 737-700 views comparisons

2.3 Geometric modelling of the Boeing 737-800

The Boeing 737-800 is an extended variant of the 737-700, taking the place of the 737-400. In terms of seating capacity, the 737-800 can accommodate 162 passengers in a two-class configuration or 189 passengers in a single-class setup.

The primary data of the components of the Boeing 737-800 is compiled in Table 2.3.

Fuselage and Cabin	**Length [m]**	**Length Nose [m]**	**Len. tail [m]**	**Cabin length [m]**	**Equivalent section diameter [m]**			
	38.02	3.99	10.601	23.42	3.76			
Wing	**Area [m^2]**	**Span [m]**	**Aspect ratio**	**Sweep angle [deg]**	**Dihedral angle [deg]**	**C_{root} [m]**	**C_{tip} [m]**	**Movables**
	124.596	34.296	9.441	33 (I panel) 26 (II panel)	6	7.59	1.215	Flaps, Slats and aileron
Horizontal tail	**Area [m^2]**	**Span [m]**	**Aspect ratio**	**Sweep angle [deg]**	**Dihedral angle [deg]**	**C_{root} [m]**	**C_{tip} [m]**	
	32.306	13.358	5.523	33	10	3.52	1.31	
Vertical tail	**Area [m^2]**	**Span [m]**	**Aspect ratio**	**Sweep angle [deg]**	**Dihedral angle [deg]**	**C_{root} [m]**	**C_{tip} [m]**	
	27.37	7.6	2.11	68(I panel) 37 (II panel)	0	8	1.4	
Nacelles and powerplants	**Engine Type**	**Engine number**	**Max TO weight [kg]**	**Length [m]**	**Nacelle diameter [m]**			
	CFM International CFM56-7	2	78245	4.1	2			

Table 2.3 - Boeing 737-800 data

The final model obtained is as follows:

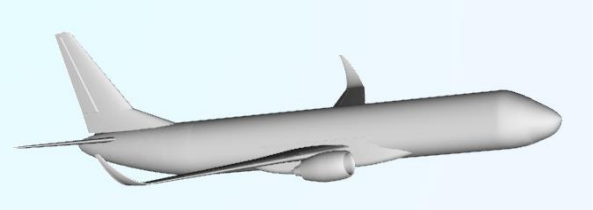

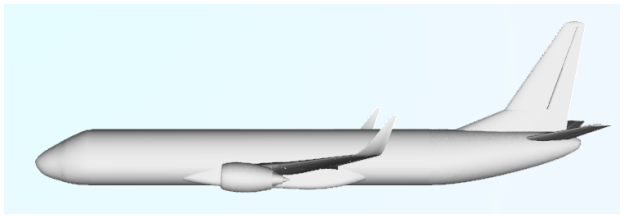

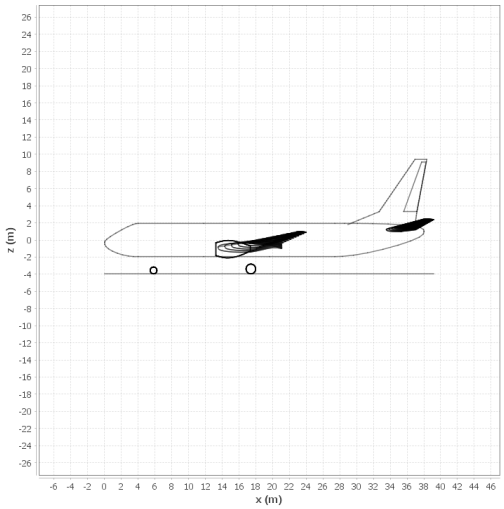

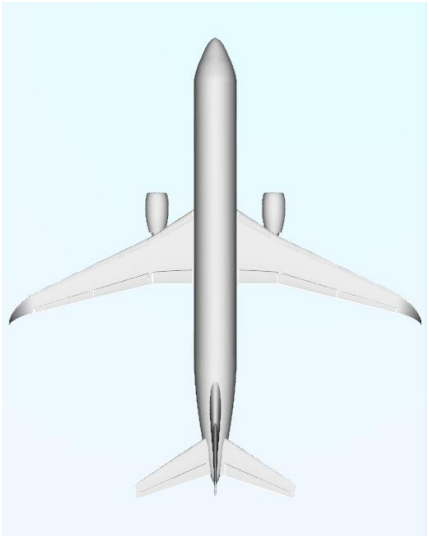

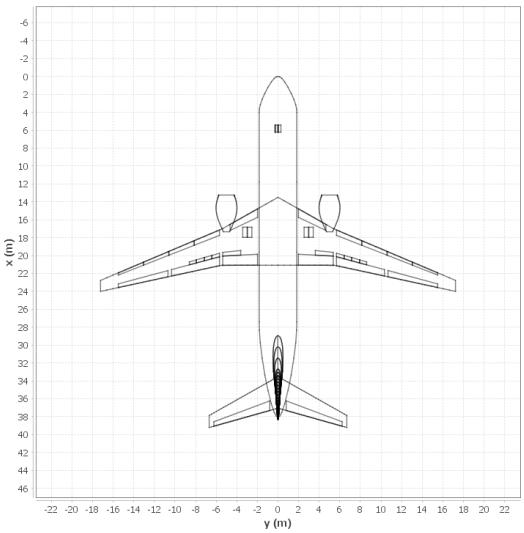

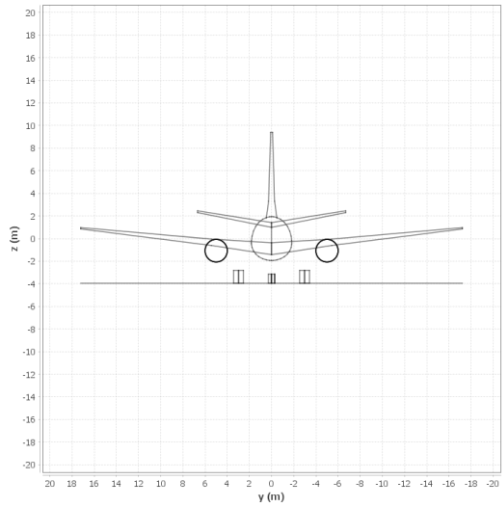

Figure 2.4 - Boeing 737-800 views comparisons

2.4 Geometric modelling of the Boeing 737-900

The Boeing 737-900 is the lengthiest within the 737 NG series: it possesses a seating capacity of 177 passengers in a dual-class layout and exceeds 189 passengers in a single-class arrangement.

The primary data of the components of the Boeing 737-900 is compiled in Table 2.4.

Fuselage and Cabin	**Length [m]**	**Length Nose [m]**	**Len. tail [m]**	**Cabin length [m]**	**Equivalent section diameter [m]**			
	40.67	3.99	10.615	26.069	3.76			
Wing	**Area [m²]**	**Span [m]**	**Aspect ratio**	**Sweep angle [deg]**	**Dihedral angle [deg]**	C_{root} **[m]**	C_{tip} **[m]**	**Movables**
	124.596	34.296	9.441	33 (I panel) 26 (II panel)	6	7.59	1.215	Flaps, Slats and aileron
Horizontal tail	**Area [m²]**	**Span [m]**	**Aspect ratio**	**Sweep angle [deg]**	**Dihedral angle [deg]**	C_{root} **[m]**	C_{tip} **[m]**	
	32.306	13.358	5.523	33	10	3.52	1.31	
Vertical tail	**Area [m²]**	**Span [m]**	**Aspect ratio**	**Sweep angle [deg]**	**Dihedral angle [deg]**	C_{root} **[m]**	C_{tip} **[m]**	
	27.37	7.6	2.11	68 (I panel) 37 (II panel)	0	8	1.4	
Nacelles and powerplants	**Engine Type**	**Engine number**	**Max TO weight [kg]**	**Length [m]**	**Nacelle diameter [m]**			
	CFM International CFM56-7	2	74389	4.1	2			

Table 2.4 - Boeing 737-900 data

The final model obtained is as follows:

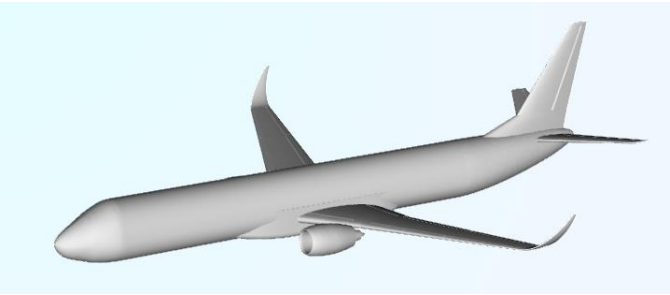

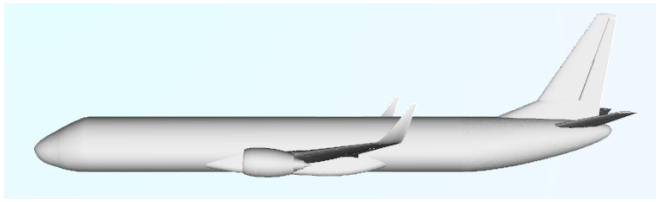

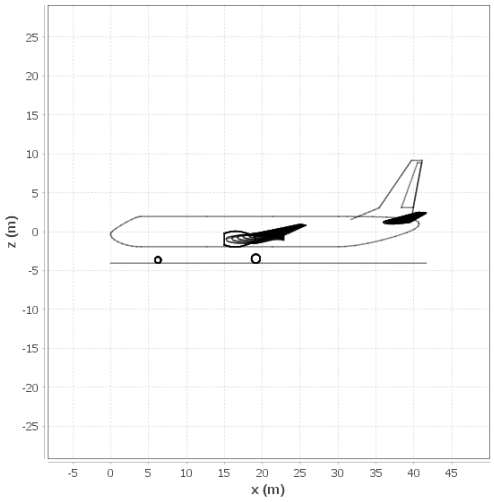

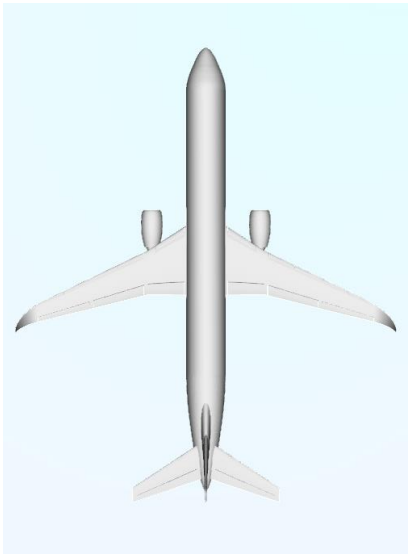

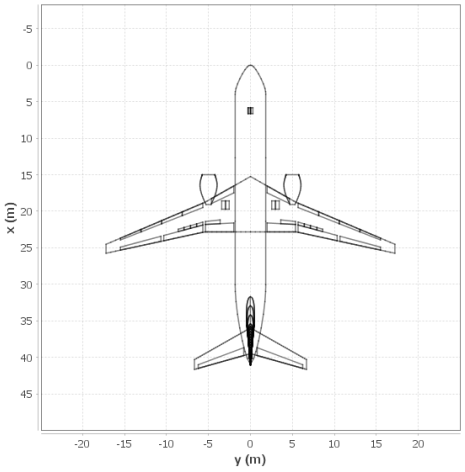

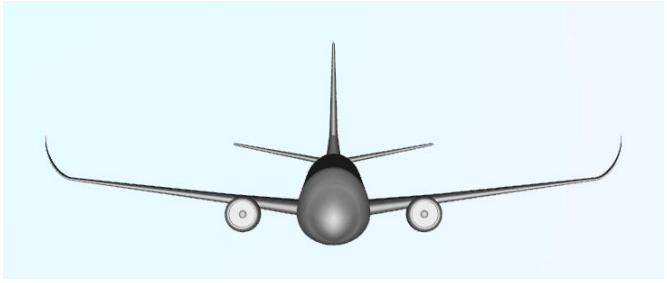

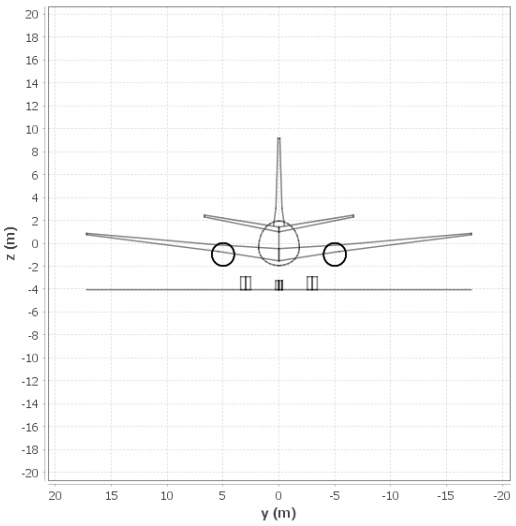

Figure 2.5 - Boeing 737-900 views comparisons

3 Analysis of performance

After the geometric modeling phase with JPAD, it was possible to carry out the performance study for the considered aircraft family.

The performance study was made possible thanks to the use of MATLAB code. Once the input data for the considered model are entered, it provides information about technical polar, propulsive characteristics, level flight, climb, descent and glide, endurance, takeoff, and landing distances.

Subsequently, the previously mentioned information is analyzed in detail for each individual model of the Boeing 737 NG aircraft family.

3.1 Data input

In the subsequent tables, the utilized input data are reported.

VERSION	AERODYNAMIC DATA						
	C_{D_O}	$C_{L_{MAX}}$	e	$C_{L_{MAX,TO}}$	$C_{L_{MAX,L}}$	C_{L_g}	M_{dd}
Boeing 737-600	0.025	1.40	0.82	1.80	2.50	0.60	0.8
Boeing 737-700	0.025	1.40	0.82	1.80	2.50	0.60	0.8
Boeing 737-800	0.025	1.40	0.82	1.80	2.50	0.60	0.8
Boeing 737-900	0.025	1.40	0.82	1.80	2.50	0.60	0.8

Table 3.1 - Aerodynamic data

Load factor $n_{max} = 2.5$

The considered cruise altitude is 10,000 m.

VERSION	WEIGHT AND GEOMETRY DATA			
	W_{TO} $[kg]$	W_f $[kg]$	S $[m^2]$	b $[m]$
Boeing 737-600	65090	20894	124.6	34.3
Boeing 737-700	69400	20894	124.6	34.3
Boeing 737-800	78245	20894	124.6	34.3
Boeing 737-900	79016	20894	124.6	34.3

Table 3.2 - Weight and geometry data

VERSION	POWERPLANT DATA		
	T_0 $[kgf]$	$TSFC$ $[\frac{lb}{lb * hr}]$	$n°$
Boeing 737-600	10000	0.36	2
Boeing 737-700	11500	0.36	2
Boeing 737-800	12000	0.36	2
Boeing 737-900	12000	0.36	2

Table 3.3 - Powerplant data

3.2 Technical polar

The characteristic points of the drag polar curve are as follows:

- Point E: point of maximum efficiency where the drag is minimum.
- Point P: point of minimum power in level flight.
- Point A: condition that maximizes the Range.
- Point S: point of minimum aircraft speed.

Below are the results evaluated at sea level and cruise altitude.

SEA LEVEL

POINT E

VERSION	C_L	C_D	E	$V\ [\frac{m}{s}]$	$T\ [N]$	$P\ [kW]$	M
Boeing 737-600	0.78	0.050	15.6	103.6	40942	4240	0.3
Boeing 737-700	0.78	0.050	15.6	106.9	43653	4660	0.31
Boeing 737-800	0.78	0.050	15.6	113.6	49216	5589	0.33
Boeing 737-900	0.78	0.050	15.6	114.1	49701	5672	0.34

Table 3.4 - Point E at sea level

POINT P

VERSION	C_L	C_D	E	$V\ [\frac{m}{s}]$	$T\ [N]$	$P\ [kW]$	M
Boeing 737-600	1.35	0.100	13.5	78.7	47275	3720	0.23
Boeing 737-700	1.35	0.100	13.5	81.3	50406	4096	0.24
Boeing 737-800	1.35	0.100	13.5	86.3	56830	4904	0.25
Boeing 737-900	1.35	0.100	13.5	86.7	57390	4977	0.25

Table 3.5 - Point P at sea level

POINT A

VERSION	C_L	C_D	E	$V\ [\frac{m}{s}]$	$T\ [N]$	$P\ [kW]$	M
Boeing 737-600	0.45	0.033	13.5	136.3	47275	6444	0.4
Boeing 737-700	0.45	0.033	13.5	140.8	50405	7095	0.41
Boeing 737-800	0.45	0.033	13.5	149.5	56830	8494	0.44
Boeing 737-900	0.45	0.033	13.5	150.2	57390	4979	0.44

Table 3.6 - Point A at sea level

POINT S

VERSION	C_L	C_D	E	$V\ [\frac{m}{s}]$	$T\ [N]$	$P\ [kW]$	M
Boeing 737-600	1.4	0.106	13.2	77.3	48154	3723	0.23
Boeing 737-700	1.4	0.106	13.2	79.8	51343	4098	0.23
Boeing 737-800	1.4	0.106	13.2	84.8	57886	4906	0.25
Boeing 737-900	1.4	0.106	13.2	85.2	58457	4979	0.25

Table 3.7 - Point S at sea level

CRUISE ALTITUDE

POINT E

VERSION	C_L	C_D	E	$V\ [\frac{m}{s}]$	$T\ [N]$	$P\ [kW]$	M
Boeing 737-600	0.78	0.050	15.6	178.5	40942	7306	0.6
Boeing 737-700	0.78	0.050	15.6	184.3	43653	8044	0.62
Boeing 737-800	0.78	0.050	15.6	195.7	49216	9630	0.65
Boeing 737-900	0.78	0.050	15.6	196.6	49701	9772	0.66

Table 3.8 - Point E at cruise altitude

POINT P

VERSION	C_L	C_D	E	$V\ [\frac{m}{s}]$	$T\ [N]$	$P\ [kW]$	M
Boeing 737-600	1.35	0.100	13.5	135.6	47276	6410	0.45
Boeing 737-700	1.35	0.100	13.5	140.0	50406	7058	0.47
Boeing 737-800	1.35	0.100	13.5	148.7	56830	8449	0.5
Boeing 737-900	1.35	0.100	13.5	149.4	57390	8578	0.5

Table 3.9 - Point P at cruise altitude

POINT A							
VERSION	C_L	C_D	E	$V\ [\frac{m}{s}]$	$T\ [N]$	$P\ [kW]$	M
Boeing 737-600	0.45	0.033	13.5	234.9	47276	11103	0.78
Boeing 737-700	0.45	0.033	13.5	242.5	50406	12224	0.81
Boeing 737-800	0.45	0.033	13.5	257.5	56830	14634	0.86
Boeing 737-900	0.45	0.033	13.5	258.8	57390	14851	0.86

Table 3.10 - Point A at cruise altitude

POINT S							
VERSION	C_L	C_D	E	$V\ [\frac{m}{s}]$	$T\ [N]$	$P\ [kW]$	M
Boeing 737-600	1.4	0.106	13.3	133.2	48154	6414	0.44
Boeing 737-700	1.4	0.106	13.3	137.5	51343	7061	0.46
Boeing 737-800	1.4	0.106	13.3	146.0	57886	8453	0.49
Boeing 737-900	1.4	0.106	13.3	146.7	58457	8578	0.49

Table 3.11 - Point S at cruise altitude

3.3 Propulsive characteristics

For the calculation of the performance, it was used the following rating:

$T = K_T \cdot T_0 \cdot \sqrt{\sigma} \cdot \phi \cdot n_{engines}$ and an altitude of 5090 m was considered.

VERSION	$T\ [kN]$	$P\ [kW]$	$Fuel\ [kg]$
Boeing 737-600	114	14189	57925
Boeing 737-700	131	16318	53297
Boeing 737-800	136	17027	55608
Boeing 737-900	136	17027	55608

Table 3.12 - Propulsive characteristics

3.4 Climb, level flight, autonomies, take-off distance, and landing distance

For the calculation of the climb rate and endurance, an altitude of 5090 m and a speed of 125 m/s were used. These top performances are obtained in different conditions (altitude, airspeed, engine rating) and cannot occur all together.

VERSION	RC_{max} $[\frac{m}{s}]$	V_{max} $[\frac{km}{h}]$	R_max $[km]$	En_max $[hr]$	Take-off field length $[m]$	Landing length $[m]$
Boeing 737-600	10.35	839	8397	16.77	1542	1217
Boeing 737-700	11.71	869	8079	15.52	1524	1295
Boeing 737-800	9.96	867	7526	13.46	1851	1386
Boeing 737-900	9.76	866	7483	13.30	1889	1393

Table 3.13 - Performance of climb, level flight, autonomies, take-off, and landing

4 Analysis of stability and control

After conducting the performance study, the models created with JPAD were exported in the OpenVSP format to enable stability and control analysis using the OPENVSP software, specifically with the use of VSPAERO.

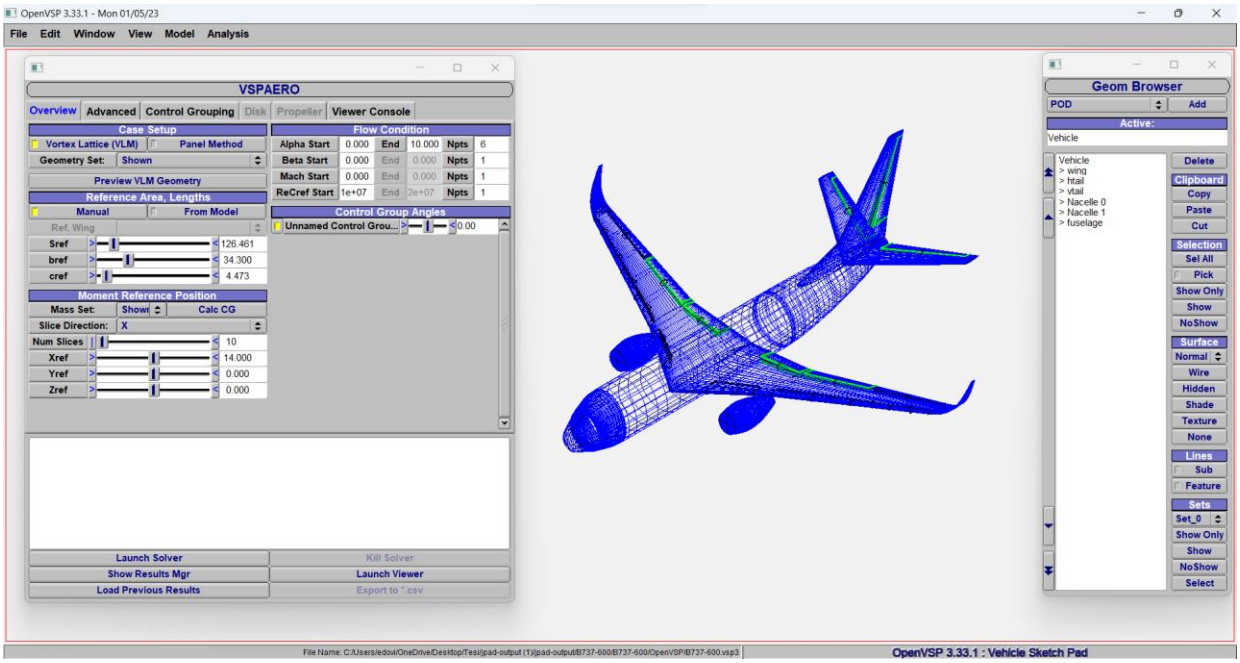

Figure 4.1 - OpenVSP interface

VSPAERO is a linear vortex lattice solver that integrates actuator disks, which can be accurately and simply described for aeropropulsive analysis. It features an interface where geometric information of the aircraft can be inputted, such as the center of gravity position, surface area, and reference chord, along with flow conditions information like Mach number, Reynolds number, and angle of attack. Once these details and the specified number of iterations (in this case, 3) are provided, the analysis can be initiated to obtain the desired results. VSPAERO does not require the indication of units of measurement; therefore, the values entered must be consistent with the measurement system selected by the user. For example, all lengths must be expressed in meters.

The following parameters were considered for the analyses:

- Variable angle of attack ranging from 0° to 10°
- Mach number at zero (no compressibility effects)
- Reynolds number at $1 \cdot 10^7$
- Fixed movable surfaces
- Reference chord (c_{ref}) of 4.473 m

- X-coordinate reference for the center of gravity varies for each model. Specifically: 14.0 m for the B737-600, 15.3 m for the B737-700, 18.5 m for the B737-800, and 20.24 m for the B737-900.

After obtaining the results of the analysis, it was possible to generate graphs. The ones that have been analyzed include: the lift curve, the drag polar curve, the pitching moment curve, the efficiency curve.

Subsequently, we will analyze each of these curves in detail.

4.1 Lift curve

The lift curve represents the relationship between the lift coefficient (C_L) and the angle of attack (a) of an aircraft. As the angle of attack increases, C_L increases linearly up to a certain point, after which it may begin to decrease or reach a maximum value. This behavior is associated with the phenomenon of stall, where the aircraft can suddenly lose lift and stability.

VSPAERO is not capable of calculating the aerodynamic stall; however, in this case, the stability derivatives of interest are obtained at small angles.

For the models considered in the analysis, the following results have been obtained and are reported in Table 4.1.

	Boeing 737-600	**Boeing 737-700**	**Boeing 737-800**	**Boeing 737-900**
$\boldsymbol{a}$ $[\boldsymbol{deg}]$		$\boldsymbol{C_L}$		
0	0.388	0.379	0.381	0.378
2	0.563	0.560	0.562	0.558
4	0.742	0.743	0.743	0.741
6	0.920	0.924	0.921	0.920
8	1.093	1.101	1.100	1.094
10	1.266	1.278	1.274	1.276

Table 4.1 - Comparison of C_L data vs Angle of attack α

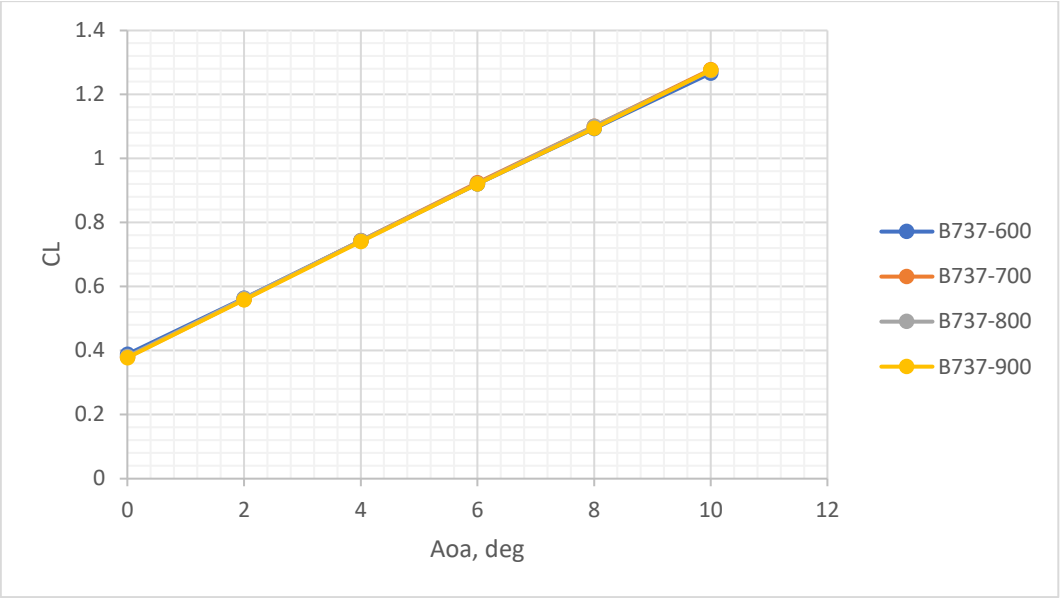

Figure 4.2 – Lift curve

It can be observed that the curves coincide.

4.2 Parabolic polar

The parabolic polar curve, also known as the polar curve, is a graph that represents the relationship between the lift coefficient (C_L) and the drag coefficient (C_D) of an aircraft. It is useful for evaluating the efficiency of the aircraft.

For the models considered in the analysis, the following results have been obtained and are reported in Table 4.2.

Boeing 737-600		**Boeing 737-700**		**Boeing 737-800**		**Boeing 737-900**	
C_L	C_D	C_L	C_D	C_L	C_D	C_L	C_D
0.388	0.015	0.379	0.016	0.381	0.016	0.378	0.015
0.563	0.023	0.560	0.023	0.562	0.023	0.558	0.022
0.742	0.033	0.743	0.032	0.743	0.032	0.741	0.032
0.920	0.046	0.924	0.045	0.921	0.045	0.920	0.044
1.093	0.062	1.101	0.060	1.100	0.060	1.094	0.059
1.266	0.081	1.278	0.078	1.274	0.078	1.276	0.077

Table 4.2 - Comparison of C_L vs C_D data

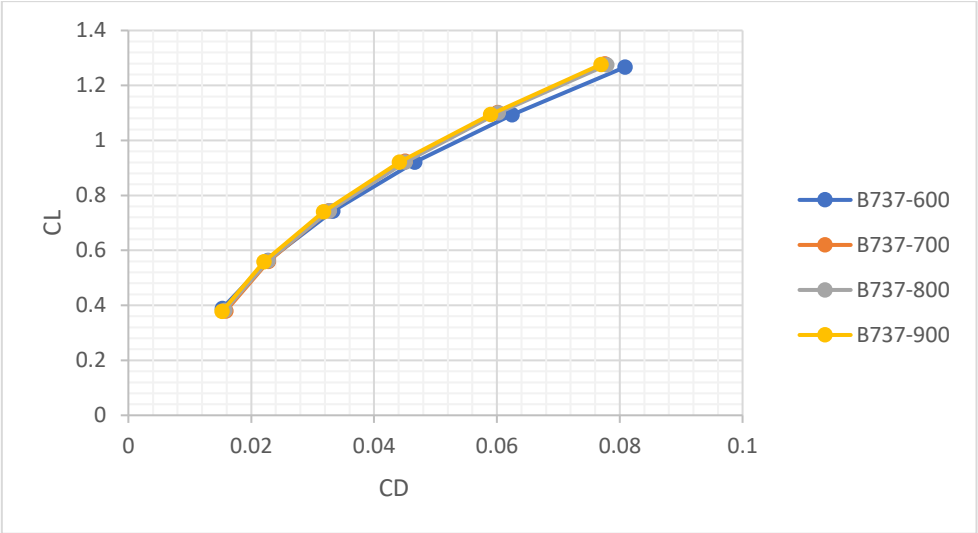

Figure 4.3 – Drag polar curves

It can be observed that the curves overlap at almost all attitudes. Note that in Chapter 3, the data reported in Table 3.1 for the evaluation of the aircraft performance were assumed to be the same among the aircraft versions. This approximation has been validated by the results of the aerodynamic analysis, with the variants with longer fuselage achieving a slightly higher lift-to-drag ratio.

4.3 Pitching moment curve

The pitching moment curve is a graph that shows how the pitching moment (C_{M_y}) varies with the angle of attack (a) of an aircraft. For longitudinal stability, this curve must have a negative slope. This means that as the angle of attack increases, the pitching moment tends to decrease. Note that the slope (i.e., the static stability margin) is function of the center of gravity position, which for all aircraft versions has been assumed to be at 30% of the root chord, with the absolute values of the CG longitudinal coordinate reported at page 24 for the different aircraft versions.

For the models considered in the analysis, the following results have been obtained and are reported in Table 4.3.

	Boeing 737-600	Boeing 737-700	Boeing 737-800	Boeing 737-900
a	C_{M_y} (ref. point at 30% wing root chord)			
0	-0.024	-0.020	0.008	0.013
2	-0.065	-0.069	-0.046	-0.041
4	-0.117	-0.123	-0.108	-0.102
6	-0.167	-0.176	-0.171	-0.160
8	-0.217	-0.229	-0.222	-0.219
10	-0.257	-0.279	-0.282	-0.279

Table 4.3 - Comparison of C_{My} data vs Angle of attack

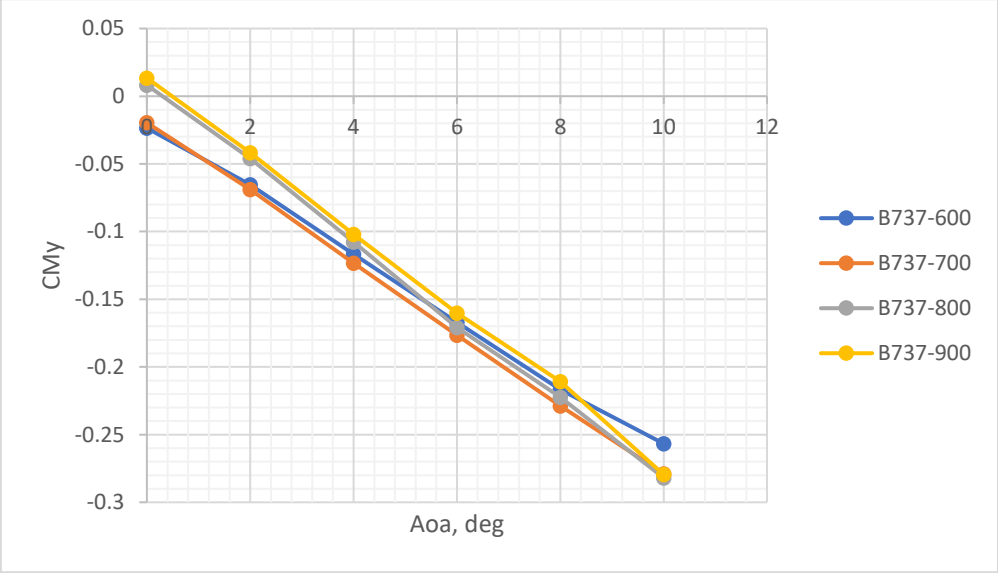

Figure 4.4 - Pitching moment curve (ref. point at 30% wing root chord)

4.4 Aerodynamic efficiency curve

The aerodynamic efficiency curve is a graph that relates the lift-to-drag ratio, *L/D*, to the angle of attack of an aircraft. The *L/D* ratio is highest at a specific angle of attack, which corresponds to the angle where the aircraft generates maximum lift relative to drag. A typical curve shows an initial increase in the *L/D* ratio as the angle of attack increases, reaches a peak, and then gradually decreases.

For the models considered in the analysis, the following results have been obtained and are reported in Table 4.4.

	Boeing 737-600	Boeing 737-700	Boeing 737-800	Boeing 737-900
a			***L/D***	
0	25.4	23.9	24.3	24.8
2	24.8	24.5	24.7	25.3
4	22.3	22.8	22.8	23.3
6	19.8	20.5	20.4	20.9
8	17.5	18.3	18.3	18.6
10	15.7	16.5	16.4	16.6

Table 4.4 - Comparison of L/D data vs Angle of attack

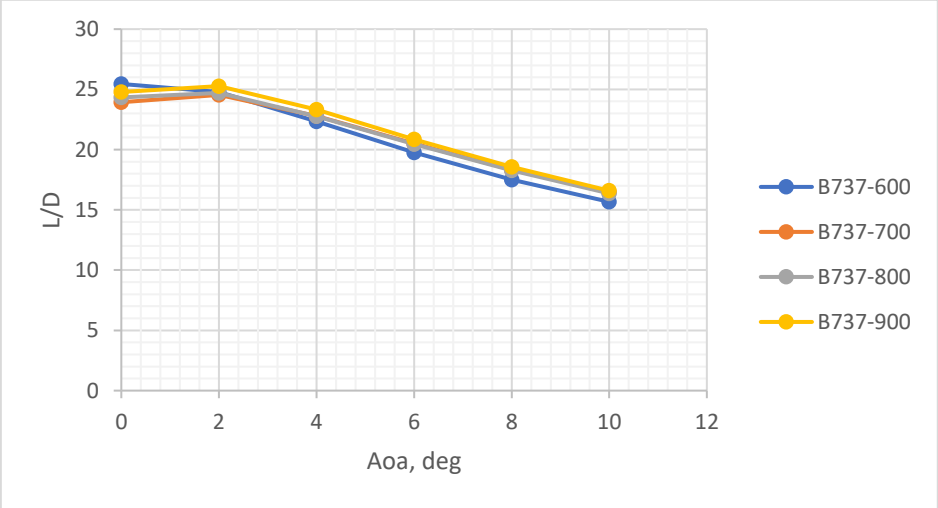

Figure 4.5 – Aerodynamic efficiency curve

4.5 Aerodynamic stability derivates

VSPAERO allows for the calculation of stability derivatives by activating the desired stability type in the "Advanced" section, in this case, "steady". Once activated, a new analysis needs to be performed, which will provide the stability derivatives. For this analysis, 5 iterations were utilized. These derivatives refer to the coefficients that represent the variation of aerodynamic forces and moments with respect to specific state parameters, such as the angle of attack.

The derivatives that have been analyzed include:

- Derivative of lift with respect to angle of attack ($dC_L/d\alpha$): represents how lift varies with changing angle of attack.
- Derivative of pitch moment with respect to angle of attack ($dC_{My}/d\alpha$): indicates how pitch moment changes with changing angle of attack.
- Derivative of roll moment with respect to sideslip angle ($dC_{Mx}/d\beta$): represents how roll moment varies with changing sideslip angle.
- Derivative of yaw moment with respect to sideslip angle ($dC_{Mz}/d\beta$): represents how yaw moment varies with changing sideslip angle.
- Derivative of pitch moment with respect to equilibrator deflection angle ($dC_{My}/d\delta_e$): provides information about the variation of moments around the longitudinal axis of the aircraft when the equilibrator is deflected.
- Derivative of yaw moment with respect to rudder deflection angle ($dC_{Mz}/d\delta_r$): provides information about the variation of moments around the z axis of the aircraft when the rudder is deflected.

The first four derivatives are stability derivatives, while the last two are control derivatives.

For the models under analysis, the following results have been obtained and are reported in Table 4.5. All the values are in rad^{-1}.

VERSION	**$dC_L/d\alpha$**	**$dC_{My}/d\alpha$**	**$dC_{Mx}/d\beta$**	**$dC_{Mz}/d\beta$**	**$dC_{My}/d\delta_e$**	**$dC_{Mz}/d\delta_r$**
Boeing 737-600	5.191	-1.31	0.222	-0.042	-1.906	-0.13
Boeing 737-700	5.20	-1.52	0.222	-0.079	-2.1	-0.14
Boeing 737-800	5.217	-1.76	0.227	-0.097	-2.490	-0.17
Boeing 737-900	5.256	-1.76	0.228	-0.113	-2.582	-0.19

Table 4.5 - Stability derivates (values in rad^{-1})

To find the neutral stability, it is necessary to calculate the neutral point. The equation below gives the expression of the neutral point:

$$\bar{x}_N \stackrel{def}{=} \frac{x_N}{\bar{c}} = \frac{\bar{x}_{ac,WB} + \eta_H \cdot \frac{C_{L\alpha,H}}{C_{L\alpha,WB}} \cdot \frac{S_H}{S} \cdot \bar{x}_{ac,H} \cdot \left[1 - \left(\frac{d\varepsilon}{d\alpha}\right)_H\right]}{1 + \eta_H \cdot \frac{C_{L\alpha,H}}{C_{L\alpha,WB}} \cdot \frac{S_H}{S} \cdot \left[1 - \left(\frac{d\varepsilon}{d\alpha}\right)_H\right]}$$

From the previous equation derives the definition of the static stability margin:

$$SM = \bar{x}_G - \bar{x}_N$$

A stable aircraft has $x_G < x_N$ hence a negative stability derivate, $C_{M_\alpha} < 0$, and a negative stability margin, $SM < 0$. The center of gravity is considered at 25% of the MAC (Mean Aerodynamic Chord).

VERSION	**SM**	x_G	x_N
Boeing 737-600	-0.252	0.25	0.502
Boeing 737-700	-0.292	0.25	0.542
Boeing 737-800	-0.326	0.25	0.576
Boeing 737-900	-0.334	0.25	0.584

Table 4.6 - Neutral point

5 Conclusion

The purpose of this work is to develop accurate geometric models for the Boeing 737 NG aircraft family using JPAD software, study the performance using MATLAB code, and analyze stability and control utilizing OPENVSP analysis.

Through the implementation of geometric models, it was possible to conduct a thorough analysis of the aircraft's aerodynamic configuration.

The expected results have been confirmed by the outcomes obtained through the evaluations of the software utilized, which demonstrates how the models of the Boeing 737 NG are efficient, safe, and stable aircraft.

It is relevant to underline that this work presents some limitations, including the determination of geometric variables of the main components of the aircraft and the acquisition of aerodynamic data such as lift and drag coefficients.

Additionally, although JPAD allows for the creation of realistic models, it should be noted that some of its functions are still limited. In particular, it is advisable to further refine the modeling of the windshield and the vertical tail, as it do not adequately integrate with the fuselage configuration due to its unique geometric characteristics.

In conclusion, this work has provided a significant contribution to the deepening of geometric modeling, performance, stability, and control of Boeing 737 NG aircraft. The analysis of these aspects has allowed for the expansion of knowledge regarding these aircraft.

Bibliography

[1] Boeing. 737NG Airplane Characteristics for Airport Planning. Boeing Commercial Airplanes. 2014. URL https://www.boeing.com/resources/boeingdotcom/commercial/airports/acaps/737NG_REVA.pdf

[2] Wikipedia. Boeing 737 Next Generation. In Wikipedia, The Free Encyclopedia. URL https://en.wikipedia.org/wiki/Boeing_737_Next_Generation

[3] Boeing Italy. 737. URL https://www.boeingitaly.it/prodotti-e-servizi/aerei-commerciali/737.page

[4] Elsevier. Table 2: Example Boeing 737 Data Table. In Elsevier Books Online. URL https://booksite.elsevier.com/9780340741528/appendices/data-a/table-2/table.htm

[5] Wikipedia. CFM International CFM56. In Wikipedia, The Free Encyclopedia. URL https://en.wikipedia.org/wiki/CFM_International_CFM56

[6] OpenVSP. OpenVSP: The Open Source Parametric Geometry Modeler. URL https://openvsp.org/

[7] SmartUp Engineering. JPAD Software. URL https://www.smartup-engineering.com/engineering/software/32-jpad